Available online at www.sciencedirect.com
ScienceDirect
Nuclear Medicine and Biology 36 (2009) 419–426
NUCLEAR MEDICINE — AND — BIOLOGY
www.elsevier.com/locate/nucmedbio

Radio-copper-labeled Cu-ATSM: an indicator of quiescent but clonogenic cells under mild hypoxia in a Lewis lung carcinoma model

Myungmi Oh[a], Takeshi Tanaka[a], Masato Kobayashi[b], Takako Furukawa[c], Tetsuya Mori[d], Takashi Kudo[b], Shigeharu Fujieda[a], Yasuhisa Fujibayashi[b,*]

[a]*Department of Otorhinolaryngology, School of Medicine, University of Fukui, Matsuoka Shimoizuki, Eiheiji-cho, Yoshida-gun, Fukui 910-1193, Japan*
[b]*Biomedical Imaging Research Center, University of Fukui, Matsuoka Shimoizuki, Eiheiji-cho, Yoshida-gun, Fukui 910-1193, Japan*
[c]*Diagnostic Imaging Group, Molecular Imaging Center, National Institute of Radiological Sciences, Anagawa 4-9-1, Chiba 263-8555, Japan*
[d]*Division of Radiological Sciences, Mallinckrodt Institute of Radiology, Washington University School of Medicine, St. Louis, MO 63110, USA*

Received 14 October 2008; received in revised form 26 December 2008; accepted 31 January 2009

Abstract

The purpose of this study is to reveal characteristics of ^{64}Cu-labeled diacetyl-bis(N^4-methylthiosemicarbazone) ([^{64}Cu]Cu-ATSM) during cell proliferation and hypoxia by autoradiography imaging and immunohistochemical staining.

Methods: The intratumoral distributions of [^{64}Cu]Cu-ATSM and [^{18}F]-2-fluoro-2-deoxy-D-gloucose ([^{18}F]FDG) in mice implanted with Lewis lung carcinoma (LLC1) tumor cells according to dual autoradiography were compared with the immunohistochemical staining patterns of proliferating markers [Ki-67 and 5-bromo-2′-deoxyuridine (BrdU)] and a hypoxic marker (pimonidazole). A clonogenic assay was performed using the cells of LLC1 tumor-implanted mice, and it was compared with the distribution of [^{64}Cu]Cu-ATSM.

Results: [^{64}Cu]Cu-ATSM mainly accumulated at the edge of tumors, whereas [^{18}F]FDG was distributed inside the tumor and inside the [^{64}Cu]Cu-ATSM accumulation. The number of Ki-67-positive cells/area tended to increase with [^{18}F]FDG accumulation and decrease with [^{64}Cu]Cu-ATSM accumulation. On the other hand, the number of BrdU-positive cells/area was negatively correlated with [^{18}F]FDG accumulation and positively correlated with [^{64}Cu]Cu-ATSM accumulation. High [^{64}Cu]Cu-ATSM accumulation was found outside the high-[^{18}F]FDG-accumulation and pimonidazole-positive regions. Colony formation ability was significantly higher in the tumor cells obtained from high-[^{64}Cu]Cu-ATSM-accumulation regions than the cells from the intermediate- and the low-accumulation regions.

Conclusion: [^{64}Cu]Cu-ATSM accumulation regions in tumor cells indicate quiescent but clonogenic tumor cells under mild hypoxia. [^{64}Cu]Cu-ATSM could play an important role in planning appropriate tumor radiotherapy.

Keywords: [^{64}Cu]Cu-ATSM; [^{18}F]FDG; Proliferation; Hypoxia; Clonogenic assay

1. Introduction

Hypoxia is a key microenvironmental factor for tumor development; not only does it stimulate angiogenesis and glycolysis for tumor expansion, but it also induces cell cycle arrest and genetic instability with tumor progression [1]. In addition, hypoxic regions in solid tumors are known to be resistant to radiotherapy as well as chemotherapy [2]. Thus, precise detection of hypoxic regions in tumors is of importance to predict tumor malignancy and therapeutic outcome.

Radio-copper-labeled Cu-diacetyl-bis(N^4-methylthiosemicarbazone) (Cu-ATSM) has been developed as a positron emission tomography (PET) agent for hypoxia imaging [3–6] as well as an internal radiotherapy agent that allows selective delivery of β-emitting Cu nuclides [7,8]. Clinical study has indicated the usefulness of radio-copper-labeled Cu-ATSM for predicting the prognosis of radiotherapy in several types of cancer [9,10]. A basic comparative study of [^{64}Cu]Cu-ATSM and immunohistochemical staining revealed that high-[^{64}Cu]Cu-ATSM regions demonstrate fewer Ki-67-positive "proliferating" cells and lower vascularity, but a slight increase in apoptotic cells (although this

* Corresponding author. Tel.: +81 776 61 8431; fax: +81 776 61 8170.
E-mail addresses: sampo@u-fukui.ac.jp (M. Oh), yfuji@u-fukui.ac.jp (Y. Fujibayashi).

0969-8051/$ – see front matter © 2009 Elsevier Inc. All rights reserved.
doi:10.1016/j.nucmedbio.2009.01.016

was less than 1%), when compared with low-[^{64}Cu]Cu-ATSM regions [11]. These findings are consistent with the known characteristics of hypoxic tumor masses.

However, we also found that intratumor [^{18}F]-2-fluoro-2-deoxy-D-gloucose ([^{18}F]FDG) uptake, an indication of glycolysis, was not positively correlated with "hypoxia" as shown by [^{64}Cu]Cu-ATSM uptake [11,12]. In addition, the intratumor distribution of [^{64}Cu]Cu-ATSM is reported to be different from that of F-18-fluoromisonidazole ([^{18}F]F-MISO), a traditional hypoxia marker [13,14]. Considering these differing findings, radio-copper-labeled Cu-ATSM might visualize different aspects of hypoxia than traditional nitroimidazole compounds such as [^{18}F]F-MISO.

Supply of oxygen as well as nutrition is limited to the range of 100 to 200 μm from the vessel, and outside this range, it should become necrotic. Positron emission tomography with 3- to 5-mm resolution cannot visualize such microenvironment; hence, the hypoxic region in the PET image should be evaluated as a mixture or an average of heterogenous phenotypes.

In the present study, we compared the intratumor distribution of [^{64}Cu]Cu-ATSM with [^{18}F]FDG, a marker of glycolysis that is known to be enhanced under hypoxic conditions, macroscopically. Pimonidazole staining was also performed as a "low-oxygen, tension-specific" probe, at macroscopic as well as microscopic levels. The intratumor distribution of the three "hypoxia"-seeking probes with different aspects was compared with immunohistochemical staining of Ki-67 and 5-bromo-2′-deoxyuridine (BrdU) to elucidate the regional proliferation status, which is considered as an important feature of tumor cells. Regional clonogenicity was also examined as another aspect of tumor cells. Based on these results, possible interpretation of PET images obtained with radiolabeled Cu-ATSM, FDG and nitroimidazole probes was discussed.

2. Materials and methods

2.1. Radiopharmaceutical synthesis

^{64}Cu was produced in a small biomedical cyclotron at the Biomedical Imaging Research Center at the University of Fukui, Japan, according to a published method [12]. [^{64}Cu]Cu-ATSM was synthesized by mixing 200 mM of glycine buffer containing ^{64}Cu and H_2ATSM in dimethyl sulfoxide (1:100 by mole ratio), as described previously [6]. The radiochemical purity of synthesized [^{64}Cu]Cu-ATSM was >99%, as evaluated by high-performance liquid chromatography (LC-10ADVP; Shimadzu, Kyoto, Japan) using a reversed-phase column (Cosmosil 5C18-AR, 4.6×50 mm+4.6×150 mm; Nacalai Tesque, Kyoto, Japan) [15]. [^{18}F]FDG was synthesized by the method of Hamacher et al. [16] with an automated [^{18}F]FDG synthesizing system (JFE, Tokyo, Japan). The specific activity of [^{64}Cu]Cu-ATSM was 56 GBq/μmol, and that of [^{18}F]FDG was 20 to 50 GBq/μmol.

2.2. Animal model

Mice were treated in accordance with the animal treatment guidelines of the University of Fukui throughout the experiments. Male C57BL/6 mice (10 weeks old, weighing 20–25 g) were obtained from Japan SLC (Shizuoka, Japan). Approximately 10^7 Lewis lung carcinoma (LLC1) cells suspended in phosphate-buffered saline (PBS) were subcutaneously implanted into the right flank of mice.

2.3. Autoradiographic study

At 3 weeks after the implantation of tumor cells, each mouse was injected intravenously with 92.5 MBq (2.5 mCi) of [^{18}F]FDG, 463 kBq (12.5 μCi) of [^{64}Cu]Cu-ATSM and BrdU (10 μg/g of body weight; Sigma-Aldrich, St Louis, MO, USA) or pimonidazole hydrochloride [1-([2-hydroxy-3-piperidinyl]propyl)-2-nitroimidazole hydrochloride] (60 μg/g of body weight, HP1-100, Hypoxyprobe-1 Kit for the detection of tissue hypoxia; CHEMICON, Temecula, CA, USA). Sixty minutes after the injection, the mice were sacrificed and the tumors were removed. The removed tumors were immediately covered with optimal cutting temperature compound and frozen in methanol cooled with dry ice. They were divided into two sections and frozen, and the cutting surfaces were flattened with a cryostat (Cryocut 1800; Leica, Wetzlar, Germany) and subjected to dual-tracer autoradiography [5]. [^{18}F]FDG images were acquired over 3 min by exposing the frozen sections to an imaging plate (BAS-MP 2040S; Fuji Photo Films, Japan) in a freezer. The imaging plate was scanned with a bioimaging analyzer (BAS-1500, Fuji Photo Films). After waiting 40 h for ^{18}F decay, [^{64}Cu]Cu-ATSM images were acquired over 45 h under frozen conditions, and the imaging plate was scanned. The distributions of [^{18}F]FDG and [^{64}Cu]Cu-ATSM were visualized by Mac-BAS v2.52 software (Fuji Photo Films). The contribution of ^{64}Cu radioactivity to the FDG image (the first autoradiography) was estimated to be around 1%, and the contribution of ^{18}F radioactivity to the Cu-ATSM image (the second exposure) was thought to be less than 0.1%. In each tumor section, the most photostimulated luminescence region was classified as 100%, and the background was defined as 0%. The 0% to 100% range was divided into four parts and colored red (75–100%), orange (50–75%), green (25–50%) and blue (0–25%), while the background was covered black. The colored image was saved in true color TIFF format.

2.4. Immunohistochemical staining with Ki-67 and BrdU

The frozen blocks used for the double tracer autoradiography were thawed, fixed in 10% neutral buffered formalin and embedded in paraffin. The sections used for the immunohistochemical staining were taken from a region 50 μm from the surface exposed for autoradiography. After ^{64}Cu decay, immunohistochemical staining was carried out to detect proliferating cells, using 4-μm-thick serial paraffin

sections. The proliferation markers used were Ki-67 and BrdU incorporation into DNA.

Ki-67 is a nuclear protein that is expressed at all active phases of the cell cycle (G_1, S, G_2 and mitosis) with its highest expression being in the G_2/M phase, but it is absent from resting cells (G_0) [16]. The proliferating cell fraction can be determined immunohistochemically by using antibodies against Ki-67. The sections were deparaffinized and rehydrated, and then endogenous peroxidase was blocked by 3% hydrogen peroxide. Antigen retrieval was carried out by microwaving for 25 min in 10 mM of citrate buffer at pH 6. Nonspecific stain-blocking reagent (X0909; Dako Cytomation, Glostrup, Denmark) was applied for 20 min at room temperature (RT). The sections were then incubated overnight at 4°C with rat monoclonal anti-mouse Ki-67 antigen antibody (M7249, Dako Cytomation) in a 1:50 dilution with PBS. After washing with PBS, the sections were incubated with rabbit anti-rat biotinylated secondary antibody (E0468, Dako Cytomation) in a 1:200 dilution with PBS for 30 min at RT before being incubated with streptavidin conjugated to horseradish peroxidase (K0673, Dako Cytomation) for 30 min at RT. Finally, the sections were incubated with 3,3′-diaminobenzine tetrahydrochloride solution (DAB liquid system, Dako Cytomation) until suitable staining developed, and then the nuclei were slightly counterstained with hematoxylin.

BrdU is a halogenated pyrimidine analogue of thymidine, which is incorporated into the DNA of proliferating cells in the S-phase; thus, it tracks the fate of dividing cells and their progeny. BrdU can be detected directly with an anti-BrdU monoclonal antibody [17,18]. It is generally used as a proliferating marker. After the sections were deparaffinized and rehydrated, endogenous peroxidase was blocked by 3% hydrogen peroxide and the sections were incubated with protease K (Wako, Japan) in 1:50,000 dilutions with PBS for 20 min at 37°C. After rinsing with PBS, the sections were incubated with 2 N HCl for 15 min at 45°C and neutralized with 0.1 M borate buffer two times at 5 min each before being rinsed with PBS containing 0.02% Tween-20, and nonspecific staining was blocked as above. The sections were incubated overnight at 4°C with mouse monoclonal antibody against BrdU (Roche Diagnostics, Switzerland) in 1:200 dilutions with PBS. After washing with PBS containing 0.05% Tween-20 (PBST-0.05%), the sections were incubated with rabbit anti-mouse biotinylated secondary antibody (Dako Envision+ Dual Link; Dako Cytomation, Japan) for 30 min at RT. After washing with PBST-0.05%, peroxidase color visualization was carried out with DAB (30 mg dissolved in 150 ml of PBST-0.05% added to 10 μl of 30% H_2O_2 solution; Dojin, Kumamoto, Japan). Counterstaining was performed as described above.

2.5. Immunohistochemical staining with a hypoxic marker

Pimonidazole hydrochloride is a bioreductive chemical probe with an immunorecognizable side chain. The addition of the first electron during bioreductive activation is reversibly inhibited by oxygen, resulting in futile cycling with a half-maximal pO_2 of inhibition of about 3 mmHg, with complete inhibition occurring at about 10 mmHg [19]. The sections were deparaffinized and rehydrated, and then endogenous peroxidase was blocked by 3% hydrogen peroxide. Nonspecific stain-blocking reagent was applied for 15 min at RT. The sections were then incubated overnight at 4°C with hypoxyprobe (hypoxyprobe Mab-1, Hypoxyprobe-1 Kit for the Detection of Tissue Hypoxia, CHEMICON) in a 1:10 dilution with PBS. After washing with PBS, the sections were incubated with rabbit anti-mouse biotinylated secondary antibody for 50 min at RT. After washing with PBS, peroxidase color visualization was carried out with DAB solution, and counterstaining was performed as described above.

2.6. Autoradiography image analyses with proliferation markers

Whole images of the serial sections stained for Ki-67, BrdU or pimonidazole were captured by a scanner (Epson GT-8500) and saved in JPEG format. Composite images were made using Adobe Photoshop to compare the autoradiographic images with those of the stained sections. [^{64}Cu]Cu-ATSM and [^{18}F]FDG images were stacked in layers above the images of stained sections and made translucent. A composite image was made for each tumor mass, and five composite images were quantified. In each composite image, three areas from the region of each color for [^{64}Cu]Cu-ATSM and [^{18}F]FDG were analyzed. Digital images of the area (0.31 mm^2) were obtained at magnification ×200 using a microscope (Olympus BX50) mounted with a CCD camera and connected to a Windows computer. Positive cells were manually counted on the computer monitor. The numbers of positively stained cells in the 15 areas (three areas from each section, one section from each of five mice) were averaged for each color indication level of [^{64}Cu]Cu-ATSM and [^{18}F]FDG accumulation.

2.7. Clonogenic assay

Lewis lung carcinoma tumor-bearing mice prepared as described above were intravenously injected with 3.7 MBq [^{64}Cu]Cu-ATSM. After 1 h, the mice were sacrificed and had their tumors removed, and two serial slices 1-mm thick were cut from each tumor mass immediately. From one slice, three to five blocks (2×2×1 mm) were cut. The blocks were minced, treated with 0.1 mg/ml collagenase II (Sigma) for 20 min at 37°C, disrupted by pipetting and filtered through a mesh to remove debris. The cells were recovered by centrifugation and resuspended in culture medium. The recovered cells were counted, and 500 cells were seeded in a 10-cm culture plate in duplicate. After 7 days, formed colonies were counted. The other slice was exposed to an imaging plate, and accumulation of [^{64}Cu]Cu-ATSM was analyzed

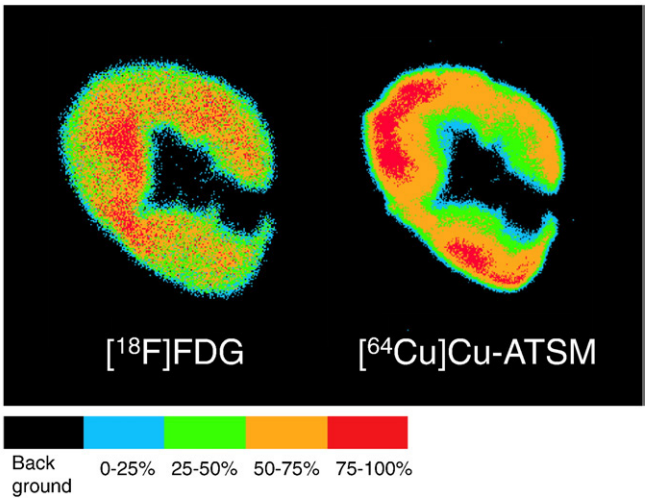

Fig. 1. Representative intratumoral distribution of [^{18}F]FDG and [^{64}Cu]Cu-ATSM in the tumor mass of LLC1. The autoradiographic images of [^{18}F]FDG and [^{64}Cu]ATSM are displayed in the same section. [^{64}Cu]Cu-ATSM is mainly accumulated at the edge of the tumors, and no accumulation is seen in the center where the cells are necrotic. The highest uptake region of [^{64}Cu]Cu-ATSM was outside that of [^{18}F]FDG.

by MacBas as described above. The positions of the blocks were referred to the [^{64}Cu]Cu-ATSM image, and [^{64}Cu]Cu-ATSM accumulation of the regions from which the blocks were cut out was determined and classified into low (in the areas colored blue to green, 0–50%), intermediate (mostly orange, 50–75%) and high (mostly red, 75–100%). Out of 18 blocks in total from four mice, five were classified as low, five as intermediate and eight as high.

Statistical analysis was performed with the Wilcoxon rank-sum test using Office Excel 2003 software (Microsoft). $P<.05$ was considered statistically significant.

3. Results

3.1. Intratumor distribution of [^{18}F]FDG and [^{64}Cu]Cu-ATSM

To analyze the intratumor distributions of [^{64}Cu]Cu-ATSM and [^{18}F]FDG, we performed dual autoradiography with mouse-implanted LLC1 tumors. Representative images are shown in Fig. 1. [^{64}Cu]Cu-ATSM mainly accumulated at

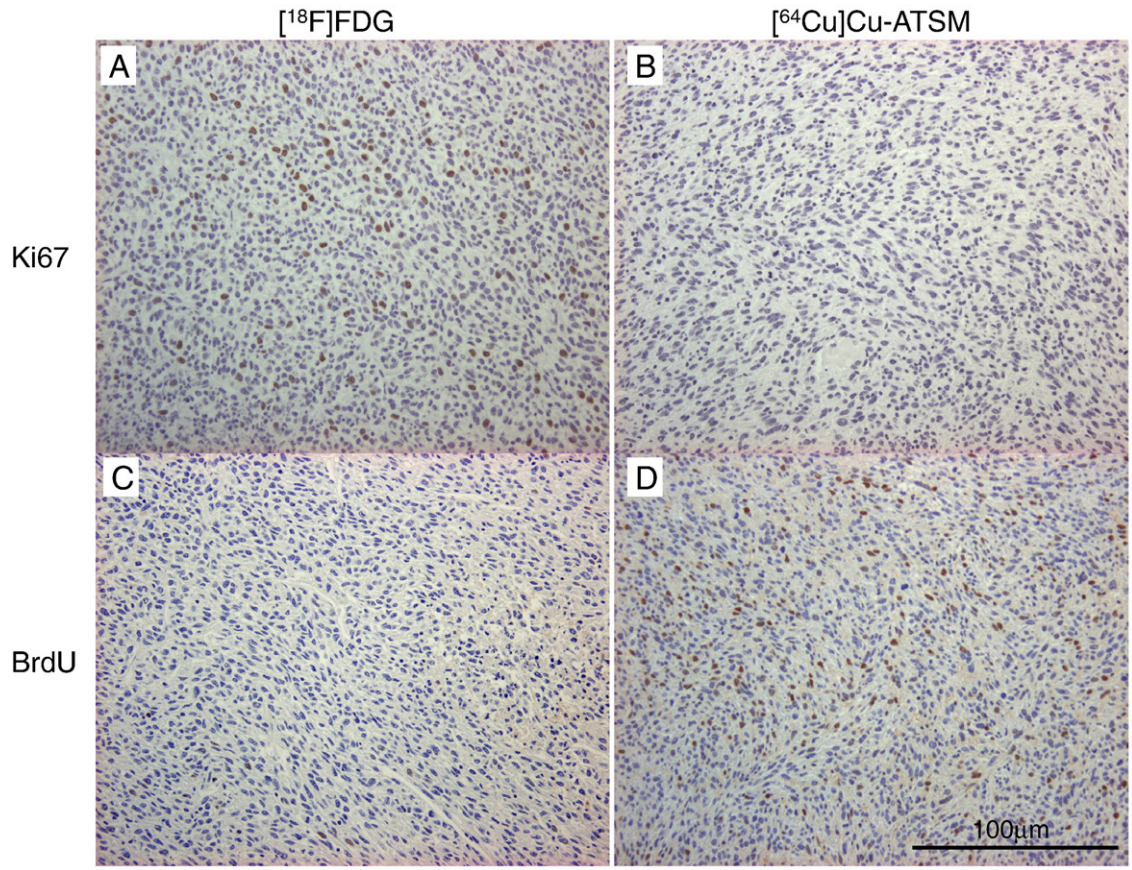

Fig. 2. Immunohistochemical staining for Ki-67 (A and B) and BrdU (C and D) in LLC1 cells at ×200. The highest [^{18}F]FDG regions are in Panels A and C, while the [^{64}Cu]ATSM regions are in Panels B and D. Positive nuclear staining of Ki-67 in tumor cells was abundantly observed in the highest [^{18}F]FDG region, but it was hardly observed in that of [^{64}Cu]Cu-ATSM. BrdU-positive cells were hardly observed in the highest [^{18}F]FDG region, but they were abundantly observed in that of [^{64}Cu]Cu-ATSM.

the edge of the tumors, and no accumulation was seen in the center where the cells were necrotic. On the other hand, the highest uptake region of [^{18}F]FDG was seen inside that of [^{64}Cu]Cu-ATSM. The most intense regions of [^{18}F]FDG and [^{64}Cu]Cu-ATSM staining, which were colored red, were distributed differently in all sections studied. These results were consistent with our previous report [11].

3.2. Autoradiography image analysis with Ki-67

To evaluate cell proliferation in each section, we performed Ki-67 and BrdU immunohistochemistry. Positive nuclear staining of Ki-67 in tumor cells was abundantly observed in the highest [^{18}F]FDG region, but it was hardly observed in that of [^{64}Cu]Cu-ATSM (Fig. 2A and B). There was a tendency for the number of Ki-67-positive cells to increase with [^{18}F]FDG uptake (Fig. 3A) and to decrease with [^{64}Cu]Cu-ATSM uptake (Fig. 3B) as in our previous report [11].

3.3. Autoradiography image analysis with BrdU

BrdU-positive cells were hardly observed in the most intensely fluorescent [^{18}F]FDG regions, but they were abundantly observed in those of [^{64}Cu]Cu-ATSM, contrary to the distribution of Ki-67-positive cells (Fig. 2C and D). There was a negative correlation between the number of BrdU-positive cells and [^{18}F]FDG uptake (Fig. 3C), and there was a positive correlation between the number of BrdU-positive cells and [^{64}Cu]Cu-ATSM uptake (Fig. 3D).

3.4. Autoradiography image analysis with pimonidazole

In LLC1 tumor, [^{18}F]FDG was distributed inside the tumor, and [^{64}Cu]Cu-ATSM was outside the distribution of [^{18}F]FDG, same as above. Fig. 4 shows an image of immunochemical staining with pimonidazole and an autoradiographic image of [^{18}F]FDG and [^{64}Cu]Cu-ATSM in LLC1 tumor. [^{18}F]FDG accumulation is distributed inside the tumor, and [^{64}Cu]

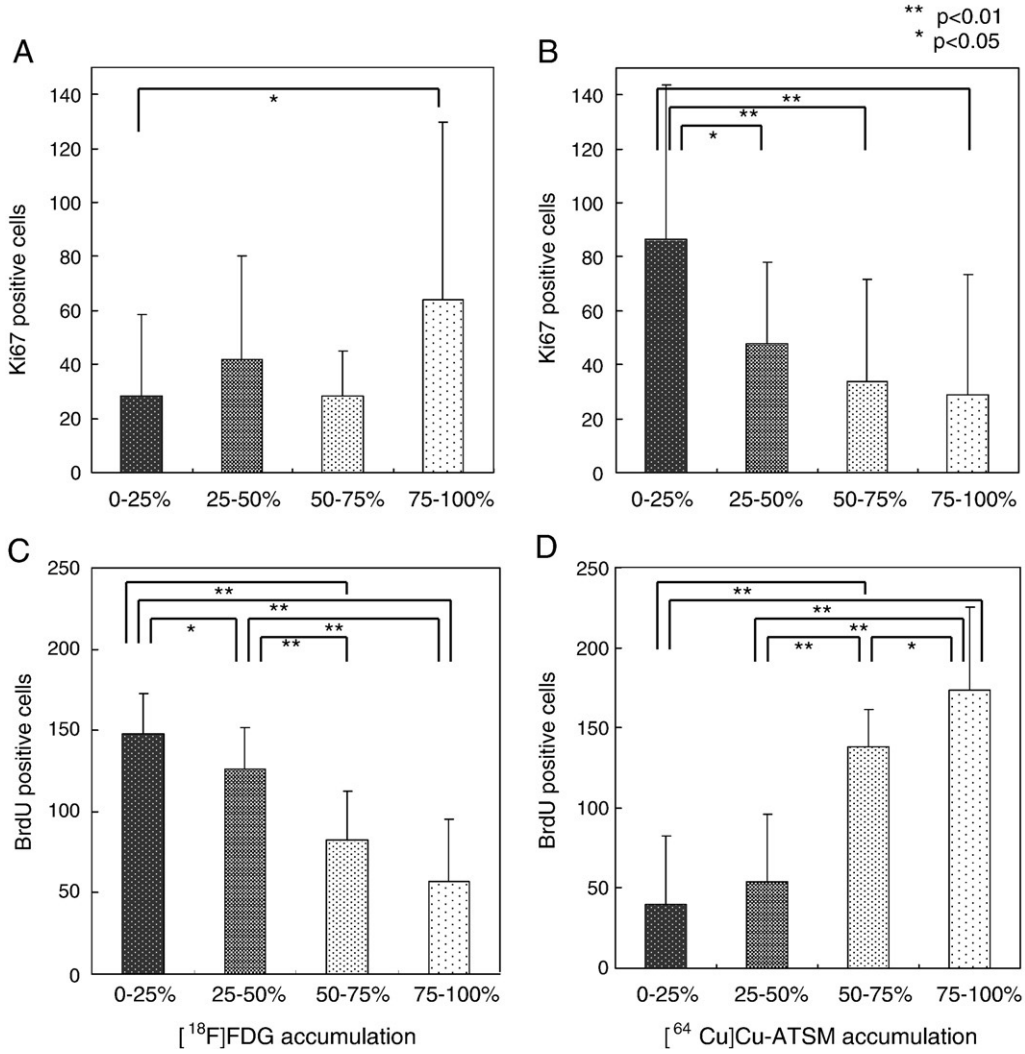

Fig. 3. Correlation between the number of Ki-67-positive (A and B) or BrdU-positive (C and D) cells and the accumulation of [^{18}F]FDG (A and C) or [^{64}Cu]ATSM (B and D). The number of Ki-67-positive cells tended to increase with [^{18}F]FDG accumulation and decrease with [^{64}Cu]Cu-ATSM accumulation. On the other hand, the number of BrdU-positive cells was negatively correlated with [^{18}F]FDG accumulation and positively correlated with [^{64}Cu]Cu-ATSM accumulation.

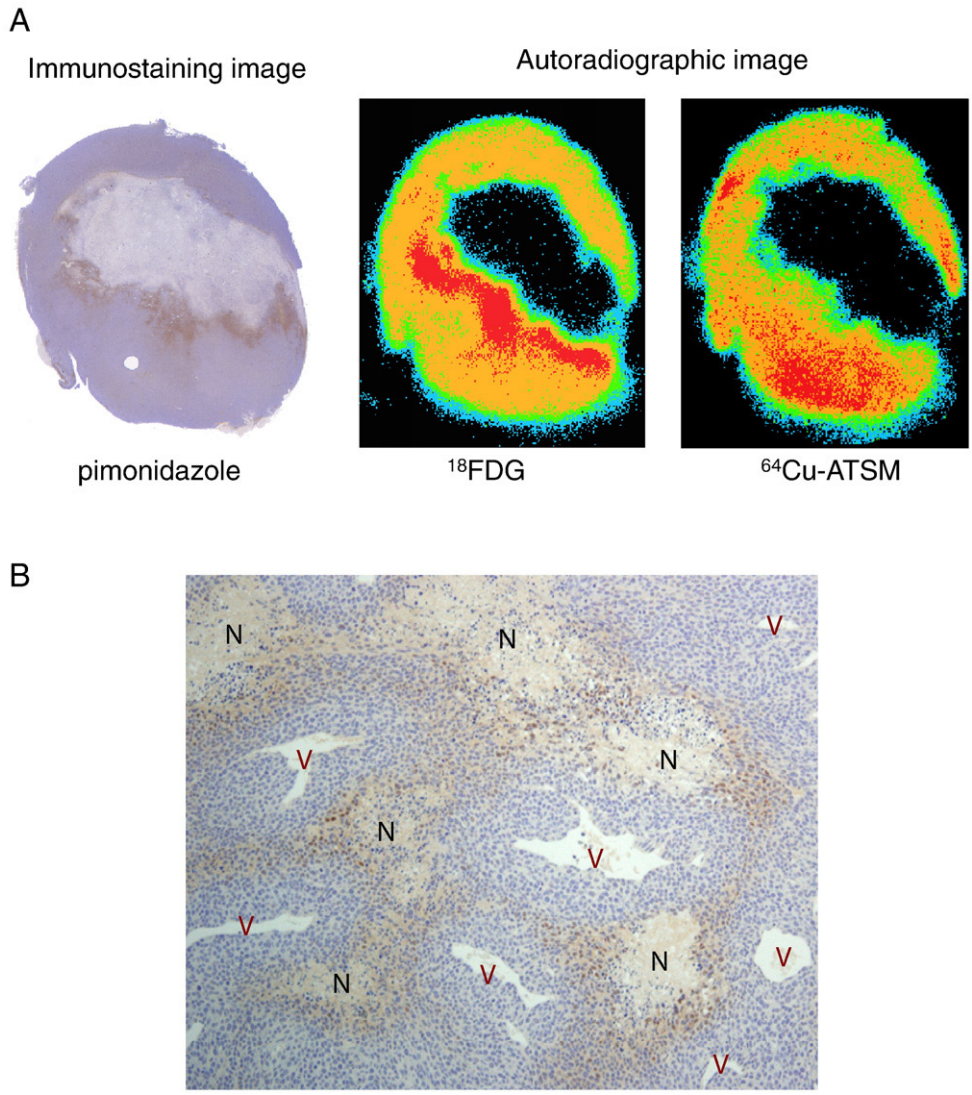

Fig. 4. An immunohistochemical staining image of pimonidazole and an autoradiographic image of [^{18}F]FDG and [^{64}Cu]Cu-ATSM at 1 h after injection into LLC1 cells. The pimonidazole staining image and the (A) autoradiographic images of [^{18}F]FDG (B) and [^{64}Cu]Cu-ATSM (C) were presented on the same slice. [^{18}F]FDG accumulation was distributed inside the tumor, and [^{64}Cu]Cu-ATSM accumulation was distributed outside the distribution of [^{18}F]FDG. The hypoxic regions shown by staining pimonidazole hydrochloride are inside the tumor and generally overlap with the distribution of [^{18}F]FDG but not [^{64}Cu]Cu-ATSM.

Cu-ATSM accumulation is distributed outside the distribution of [^{18}F]FDG. Pimonidazole hydrochloride staining of hypoxic regions is shown inside the tumors and generally lapped over the distribution of [^{18}F]FDG, but not [^{64}Cu]Cu-ATSM at 1 h postinjection of the radiotracers.

3.5. Clonogenic assay

Proliferation potential of the cells in LLC1 tumor masses was assessed by a colony formation assay. Table 1 shows the number of colonies formed from the cells recovered from the regions of high, intermediate and low accumulation of [^{64}Cu]Cu-ATSM. The number was significantly higher in the high-[^{64}Cu]Cu-ATSM-accumulation region than in the intermediate- and the low-accumulation regions ($P<.05$), indicating that the region of high [^{64}Cu]Cu-ATSM accumulation had a higher proliferation potential than the other regions.

Table 1
Colony formation ability of LLC1 tumor cells from various regions

[^{64}Cu]Cu-ATSM accumulation	No. of regions	No. of colonies formed/100 cells (average±S.D.)
High	8	20.1±3.2[a]
Medium	5	14.5±4.0
Low	5	12.9±5.1

[a] The number of colonies in the high-[^{64}Cu]Cu-ATSM-accumulation region was significantly higher than that in the intermediate- and the low-accumulation regions ($P<.05$).

4. Discussion

Copper-ATSM is a stable Cu(II) complex with high membrane permeability and is able to pass through the cell membrane between the blood and tissues instantly. Under abnormally high-NADH conditions such as hypoxia, however, Cu(II) in the Cu(II)-ATSM complex can be easily reduced to Cu(I) by a mitochondrial electron transport enzyme (NADH dehydrogenase) in an NADH-dependent manner. Hypoxia-selective reduction occurs in tumor cells also [4], but reduction in tumors is mediated by microsome fraction, not by mitochondria [20]. Microsomal reduction of Cu-ATSM is regulated by NADH-cytochrome *b*5 reductase and/or NADPH-cytochrome P450 reductase in an NADH/NADPH-dependent manner, and reduced Cu(I) is instantly dissociated from ATSM and retained within the cells. Thus, the key to Cu-ATSM retention is not considered to be oxygen tension itself, but rather a high NADH/HADPH concentration mostly, which occurs as a result of hypoxia.

Also, in the case of nitroimidazole compounds such as pimonidazole, reductive activation is ubiquitously performed by redox enzymes in an NADH/NADPH-dependent manner [21]. However, the produced nitro anion radical can be easily reoxidized under normoxic conditions [22,23]. As a result, retention of nitroimidazole is regulated by oxygen tension but is independent of NADH/NADPH redox state. From these points of consideration, Cu-ATSM and pimonidazole show completely different aspects of hypoxic tumor cells, namely, the highly reduced status and low oxygen tension within the cells, respectively.

At the macroscopic level shown in Fig. 4, pimonidazole staining showed an almost identical pattern to those of [^{18}F]FDG at 1 h postinjection. The necrotic region (no staining, no [^{18}F]FDG uptake) was surrounded by a hypoxic region (pimonidazole positive, high [^{18}F]FDG uptake) and then by a normoxic region (pimonidazole negative, moderate [^{18}F]FDG uptake). The key point here is that the distances between necrosis–hypoxia–normoxia were more than 1 to 3 mm. However, the pimonidazole-positive region was not homogenous but a network of blood vessels surrounded by proliferating tumor cells, hypoxic tumor cells and necrosis. This patchy pattern is repeated within 100 to 200 μm, known as the distance that is penetrable by oxygen. From this finding, the "hypoxic" region detected by PET using radiolabeled nitroimidazole compounds and [^{18}F]FDG is not a homogenously hypoxic region but rather is a mixture of rapidly proliferating tumor cells, hypoxic nonproliferating cells and necrosis. High accumulation of radiolabeled nitroimidazole compounds is considered to only occur in hypoxic nonproliferating cells. [^{18}F]FDG accumulation is considered to be enhanced in both regions of normoxic proliferating cells and hypoxic nonproliferating cells, because of high demand of energy for proliferation and anaerobic glycolysis, respectively. From these findings, it is indicated that "hypoxia" imaging with PET using [^{18}F]FDG or [^{18}F]F-MISO does not simply visualize hypoxic cells, but a mixture of various types of cells in tumor masses, including cells under low oxygen tension. In addition, high [^{64}Cu]Cu-ATSM accumulation at 1 h postinjection was found outside the high-[^{18}F]FDG/pimonidazole-positive region. This result corresponded with our previous report using [^{64}Cu]Cu-ATSM and [^{18}F]FDG [11]. Considering the high [^{64}Cu]Cu-ATSM uptake, lack of pimonidazole staining and the retention mechanisms of both agents, this region is thought to be in an extremely reductive condition, but not severe hypoxia.

In Fig. 2, BrdU-positive cells were hardly observed in the high-[^{18}F]FDG regions but were observed in the high-[^{64}Cu]Cu-ATSM regions, indicating that cells with a high [^{64}Cu]Cu-ATSM uptake have the ability to synthesize DNA but not during the proliferation process. BrdU is used for the detection of cell proliferation by means of DNA synthesis, especially the detection of S-phase cells. Ki-67 is also reported as a marker of proliferation, and it expresses all phases of proliferation except for G_0. However, the expression of Ki-67 varies in intensity throughout the cell cycle, and this has raised concern that it could lead to a misclassification of cycling cells as the resting ones [24]. The levels of Ki-67 are low during the G_1- and early S-phase and progressively increase to reach their maximum during mitosis [24]. van Dierendonck et al. [25] noted that some BrdU-positive cells are Ki-67 negative, although all BrdU-positive cells are thought to be Ki-67 positive. This is probably due to methodological bias [26]. In addition, mild hypoxia (ca. 1%) shows transient increases in the number of BrdU-positive cells [27], and some cancer cell lines are able to continue BrdU incorporation for as long as 24 to 48 h under these conditions [28].

Pooling these findings, it can be suggested that the cells in high-[^{64}Cu]Cu-ATSM regions were quiescent but continued DNA synthesis and that this status was induced by mild hypoxia. Extracellular conditions were considered to be rather similar within the wide range of regions because of the quiescence of the cells. This type of cells remained sensitive to progression factors; the cells obtained from a high-[^{64}Cu]Cu-ATSM region showed a high clonogenic ability under optimal growth conditions (Table 1). Therefore, the [^{64}Cu]Cu-ATSM accumulation regions were considered to be clonogenic tumor cells. These tumor cells should be attacked with [^{64}Cu]Cu-ATSM internal radiotherapy and/or X-ray external radiotherapy, such as intensity-modulated radiation therapy. On the other hand, in high-[^{18}F]FDG and pimonidazole-positive regions, complex cell populations existed; some were actively proliferating, but the large oxygen gradient from blood vessels to areas of necrosis might induce a wide variety of proliferation statuses/abilities within the cells. As a result, the overall clonogenic ability of high-[^{18}F]FDG areas was lower than that of high-[^{64}Cu]Cu-ATSM regions.

5. Conclusion

We have demonstrated that regions of accumulation of [^{64}Cu]Cu-ATSM indicate quiescence in tumor cells and clonogenic tumor cells under mild hypoxia in an LLC1-bearing animal model. [^{64}Cu]Cu-ATSM would be a tool to provide information on disease prognosis and radiotherapy planning, though further basic as well as clinical studies would be needed to clarify its precise usefulness.

Acknowledgments

The authors thank Shingo Kasamatsu, Satonao Nakakoji and the rest of the staff of the Biomedical Imaging Research Center and Nobuo Takimoto of the Department of Pathology at the University of Fukui, Japan. This study was partly funded by a Grant-in-Aid in Scientific Research from the Japan Society for the Promotion of Science (20791185) and the 21st Century COE Program (Medical Science).

References

[1] Hammer S, To KK, Yoo YG, Koshiji M, Huang LE. Hypoxic suppression of the cell cycle gene CDC25A in tumor cells. Cell Cycle 2007;6:1919–26.
[2] Wouters A, Pauwels B, Lardon F, Vermorken JB. Review: implications of in vitro research on the effect of radiotherapy and chemotherapy under hypoxic conditions. Oncologist 2007;12:690–712.
[3] Takahashi N, Fujibayashi Y, Yonekura Y, Welch MJ, Waki A, Tsuchida T, et al. Evaluation of 62Cu labeled diacetyl-bis(N^4-methylthiosemicarbazone) as a hypoxic tissue tracer in patients with lung cancer. Ann Nucl Med 2000;14:323–8.
[4] Lewis JS, McCarthy DW, McCarthy TJ, Fujibayashi Y, Welch MJ. Evaluation of 64Cu-ATSM in vitro and in vivo in a hypoxic tumor model. J Nucl Med 1999;40:177–83.
[5] Fujibayashi Y, Cutler CS, Anderson CJ, McCarthy DW, Jones LA, Sharp T, et al. Comparative studies of Cu-64-ATSM and C-11-acetate in an acute myocardial infarction model: ex vivo imaging of hypoxia in rats. Nucl Med Biol 1999;26:117–21.
[6] Fujibayashi Y, Taniuchi H, Yonekura Y, Ohtani H, Konishi J, Yokoyama A. Copper-62-ATSM: a new hypoxia imaging agent with high membrane permeability and low redox potential. J Nucl Med 1997;38:1155–60.
[7] Obata A, Kasamatsu S, Lewis JS, Furukawa T, Takamatsu S, Toyohara J, et al. Basic characterization of 64Cu-ATSM as a radiotherapy agent. Nucl Med Biol 2005;32:21–8.
[8] Lewis J, Laforest R, Buettner T, Song S, Fujibayashi Y, Connett J, et al. Copper-64-diacetyl-bis(N^4-methylthiosemicarbazone): an agent for radiotherapy. Proc Natl Acad Sci USA 2001;98:1206–11.
[9] Dehdashti F, Grigsby PW, Mintun MA, Lewis JS, Siegel BA, Welch MJ. Assessing tumor hypoxia in cervical cancer by positron emission tomography with 60Cu-ATSM: relationship to therapeutic response-a preliminary report. Int J Radiat Oncol Biol Phys 2003;55:1233–8.
[10] Chao KS, Bosch WR, Mutic S, Lewis JS, Dehdashti F, Mintun MA, et al. A novel approach to overcome hypoxic tumor resistance: Cu-ATSM-guided intensity-modulated radiation therapy. Int J Radiat Oncol Biol Phys 2001;49:1171–82.
[11] Tanaka T, Furukawa T, Fujieda S, Kasamatsu S, Yonekura Y, Fujibayashi Y. Double-tracer autoradiography with Cu-ATSM/FDG and immunohistochemical interpretation in four different mouse implanted tumor models. Nucl Med Biol 2006;33:743–50.
[12] Obata A, Yoshimoto M, Kasamatsu S, Naiki H, Takamatsu S, Kashikura K, et al. Intra-tumoral distribution of (64)Cu-ATSM: a comparison study with FDG. Nucl Med Biol 2003;30:529–34.
[13] O'Donoghue JA, Zanzonico P, Pugachev A, Wen B, Smith-Jones P, Cai S, et al. Assessment of regional tumor hypoxia using 18F-fluoromisonidazole and 64Cu(II)-diacetyl-bis(N^4-methylthiosemicarbazone) positron emission tomography: comparative study featuring microPET imaging, Po2 probe measurement, autoradiography, and fluorescent microscopy in the R3327-AT and FaDu rat tumor models. Int J Radiat Oncol Biol Phys 2005;61:1493–502.
[14] Matsumoto K, Szajek L, Krishna MC, Cook JA, Seidel J, Grimes K, et al. The influence of tumor oxygenation on hypoxia imaging in murine squamous cell carcinoma using [64Cu]Cu-ATSM or [18F] Fluoromisonidazole positron emission tomography. Int J Radiat Oncol Biol Phys 2007;30:873–81.
[15] Scholzen T, Gerdes J. The Ki-67 protein: from the known and the unknown. J Cell Physiol 2000;182:311–22.
[16] Hamacher K, Coenen HH, Stöcklin G. Efficient stereospecific synthesis of no-carrier-added 2-[18F]-fluoro-2-deoxy-D-glucose using aminopolyether supported nucleophilic substitution. J Nucl Med 1986;27:235–8.
[17] Gratzner HG. Monoclonal antibody to 5-bromo- and 5-iododeoxyuridine: a new reagent for detection of DNA replication. Science 1982;218:414–5.
[18] Riccardi A, Danova M, Ascari E. Bromodeoxyuridine for cell kinetic investigations in humans. Haematologica 1988;73:423–30.
[19] Ljungkvist AS, Bussink J, Rijken PF, Raleigh JA, Denekamp J, Van Der Kogel AJ. Changes in tumor hypoxia measured with a double hypoxic marker technique. Int J Radiat Oncol Biol Phys 2000;48:1529–38.
[20] Obata A, Yoshimi E, Waki A, Lewis JS, Oyama N, Welch MJ, et al. Retention mechanism of hypoxia selective nuclear imaging/radiotherapeutic agent Cu-diacetyl-bis(N^4-methylthiosemicarbazone) (Cu-ATSM) in tumor cells. Ann Nucl Med 2001;15:499–504.
[21] Moreno SN, Mason RP, Muniz RP, Cruz FS, Docampo R. Generation of free radicals from metronidazole and other nitroimidazoles by *Tritrichomonas foetus*. J Biol Chem 1983;258:4051–4.
[22] Arteel GE, Thurman RG, Yates JM, Raleigh JA. Evidence that hypoxia markers detect oxygen gradients in liver: pimonidazole and retrograde perfusion of rat liver. Br J Cancer 1995;72:889–95.
[23] Arteel GE, Thurman RG, Raleigh JA. Reductive metabolism of the hypoxia marker pimonidazole is regulated by oxygen tension independent of the pyridine nucleotide redox state. Eur J Biochem 1998;253:743–50.
[24] Urruticoechea A, Smith IE, Dowsett M. Proliferation marker Ki-67 in early breast cancer. J Clin Oncol 2005;23:7212–20.
[25] van Dierendonck JH, Keijzer R, van de Velde CJ, Cornelisse CJ. Nuclear distribution of the Ki-67 antigen during the cell cycle: comparison with growth fraction in human breast cancer cells. Cancer Res 1989;49:2999–3006.
[26] Du Manoir S, Guillaud P, Camus E, Seigneurin D, Brugal G. Ki-67 labeling in postmitotic cells defines different Ki-67 pathways within the 2c compartment. Cytometry 1991;12:455–63.
[27] Green SL, Freiberg RA, Giaccia AJ. p21(Cip1) and p27(Kip1) regulate cell cycle reentry after hypoxic stress but are not necessary for hypoxia-induced arrest. Mol Cell Biol 2001;21:1196–206.
[28] Denko NC, Green SL, Edwards D, Giaccia AJ. p53 checkpoint-defective cells are sensitive to X rays, but not hypoxia. Exp Cell Res 2000;258:82–91.